

FILE COPY

Columbia University  
PALISADES, NEW YORK

Lamont Geological Observatory

Holzer 5

# Technical Report on Seismology

No. 9

Crustal Structure Beneath the Gulf of Maine



Lamont Geological Observatory

(Columbia University)

Palisades, New York

CRUSTAL STRUCTURE BENEATH THE GULF OF MAINE

Technical Report No. 9

by

Samuel Katz

Samuel Katz

Richard S. Edwards

Richard S. Edwards

Frank Press

Frank Press

The research reported in this document has been made possible through support and sponsorship extended by the Geophysical Research Directorate of the Cambridge Field Station, AMC, U. S. Air Force, under Contract W-28-099 ac-396, by the Office of Naval Research under Contract N6-onr-271, Task Order XIII, and by the Woods Hole Oceanographic Institution. It is published for technical information only and does not represent recommendations or conclusions of the sponsoring agencies.

December 1950

## ABSTRACT

Seismic refraction profiles obtained by ship-to-shore recording in the Gulf of Maine, and the velocity distribution in the upper part of the earth's crust, inferred from these profiles, are described. The surface layer has a velocity of 5.34 km/sec, and extends down to a depth of 5.1 km at Falmouth, Maine. Beneath, a layer with a velocity of 6.25 km/sec is found to slope upward to the east at  $3^{\circ}$  over a distance of at least 80 km. A layer with a velocity of 7.5 km/sec appears at a depth of 16.7 km at Falmouth, Maine. The unusual submarine topography beneath the course of the shot boat is illustrated.

## TABLE OF CONTENTS

- I Introduction
- II Falmouth to Mt. Desert Island Profile
  - a. Data
  - b. Interpretation
- III Mt. Desert Island to Crowell Profile
- IV Comparison with other Investigations
- V Depth Soundings

## FIGURES

- I Index Map
- II Seismograms
- III Falmouth Travel Time Curve
- IV Mt. Desert Island Travel Time Curve
- V Travel Time Curves for Dipping Bed as Function of Azimuth
- VI Original and Corrected Crowell Travel Time Curve
- VII Corrected Mt. Desert Island Travel Time Curve
- VIII Crustal Columns
- IX Bottom Topography along Shot Course

## TABLES

- I Shot Times and Positions
- II Data for Falmouth, Mt. Desert Island, and Crowell
- III Computed Compared with Observed Travel Times

#### ACKNOWLEDGMENTS

The authors wish to express their appreciation to P. J. Coyle, T. S. Crane, J. G. Heacock, Jr., G. L. Shurbet, E. B. Walden, and J. L. Worzel for their participation in the recording program; and to T. R. Madden, John Northrop, and G. H. Sutton for their part in the work of detonating and timing the depth charges, and navigating aboard the USS Mentor.

Professor W. M. Ewing suggested the method used for interpreting the data and gave other valuable advice. Mrs. Marie Flanagan prepared the drawings and Miss J. B. Parker helped in the computations. To all these, the authors are very grateful.

## I Introduction

On August 11, 1949, the USS Mentor (PYC) steamed eastward across the Gulf of Maine on the course shown in Figure I, and detonated 300-pound depth charges at half-hour intervals. The shot times and positions are given in Table I. Three portable seismograph stations recorded the seismic waves generated by these explosions. The locations of these stations at Falmouth near Portland, Maine, on Mt. Desert Island, Maine, and at Crowell, Nova Scotia, are also shown in Figure I. A fourth station located on a vessel off Matinicus Rock was inoperative because of equipment failure.

Between the Portland Lightship and Matinicus Rock, including shots 1 through 13, the course was well marked by several fixes on buoys and prominent shore marks. On this portion of the course, the seismic results and the interpretation based on a modified reverse profile are fairly reliable. However, east of Matinicus Rock, neither visual nor Loran fixes could be obtained and the navigation, based on previously determined speed, was entirely by dead reckoning. The failure of one of its engines prevented the Mentor from continuing its run across the Gulf of Maine and obtaining a fix at the Lurcher Shoal Light, the eastern end of the course. Therefore, on this portion of the course the seismic results are subject to considerable uncertainty.

The recording station instruments, including seismometers, amplifiers, chronometers, radios, and power supply, as well as recording procedures, are described by Luskin et al. in Technical Report No. 10. Typical seismograms obtained at each recording station at various distances are shown in Figure II.

## II Falmouth to Mt. Desert Island Profile

### a. Data

The data obtained by the Falmouth and Mt. Desert Island recording stations are shown in Columns 1 and 2 of Table II and Figures III and IV.

The travel times of shots 1 and 2 at Falmouth, together with the origin, indicate a surface layer with a velocity of 5.34 km/sec. Beyond shot 2 occurs the first break in the travel time curve. The combined data of the Falmouth and Mt. Desert Island stations indicate that the refracting surface has a small dip to the west. Since these two stations were not in line with the course of the shot boat, a simple reverse profile could not be worked out. This will be discussed further below. However, the dip is small, and the stations were not far off the shot course; hence, we may use a straight line\* to represent the portion of the Falmouth travel time curve between shots 3 (36.6 km) and 11 (97 km):

$$T = \frac{X}{6.49} + 1.0$$

where X and T are in kilometers and seconds, respectively. The apparent velocity is 6.49 km/sec ; the intercept 1.0 sec. At a distance of 103.8 km, there is a further break in the travel time curve. The travel time for shots 13 through 15 is:

$$T = \frac{X}{7.54} + 3.4$$

giving a velocity of 7.54 km/sec and an intercept of 3.4 seconds.

-----

\* For the method of analyzing the data, see Wald (1940).

The Mt. Desert Island travel-time curve (Figure IV) consists of two branches, the shots to the west of the recording station falling along the upper branch (shots 5 through 14). The travel time for this branch is

$$T = \frac{X}{6.09} + .38$$

giving an apparent velocity of 6.09 km/sec and a time intercept of .38 seconds. The lower branch of the curve will be discussed in Section III.

#### b. Interpretation

As indicated, when the recording stations are not in line with the course of the shooting boat, the interpretation can no longer be made along the lines of a simple reverse profile, because for each recording station the travel time is a function of the bearing of the shot, of the dip, strike, depth and velocity of the refracting layer, and of the horizontal distance between recorder and shot. Although no direct analytical or geometrical means for computing these quantities from the observed travel time curves has yet been found, a relatively simple method, suggested by Professor M. Ewing, has been developed and used for this purpose.

It may easily be shown (see Appendix) that for the two layer case, with a compressional wave velocity  $V_1$  for the upper layer,  $V_2$  and dip angle  $d$  for the lower layer, the general travel time for a refracted seismic wave is

$$T = \frac{X}{V_1} \sin(i \pm n) + \frac{2D \cos i}{V_1} \quad (1)$$

Here  $n$ , the apparent dip angle at azimuth  $a$ , is given by

$$n = \text{arc sin } (\cos a \sin d)$$

where  $\underline{a}$  is measured from the dip line drawn up-slope through the fixed station (the recording station in this case) and the critical angle of refraction is

$$i = \text{arc sin } \frac{V_1}{V_2}$$

$D$  is the perpendicular distance of the fixed station to the refracting horizon. The minus sign is used when the moving station (the shot boat in this case) is up-slope from the fixed station.

Defined as the reciprocal of the slope at a particular point of the travel-time curve between a fixed and a movable station, the apparent velocity  $V_a$  is obtained from (1) and is given by

$$V_a = \frac{V_1}{\sin(i \pm n)} \quad (2)$$

It should be noted that in the conventional case of shot course in line with the receiving station (or the geophone spread in line with the shot) the apparent velocity of a plane refracting horizon is constant (i.e. a straight line). On the other hand, in this case, as a result of its dependence on the azimuth  $\underline{a}$  through the apparent dip angle  $\underline{n}$ , the apparent velocity  $V_a$  changes from point to point along the travel-time curve.

By plotting a family of curves of  $V_a$  as a function of  $\underline{a}$ , for an assumed set of values  $V_1$ ,  $V_2$ , and  $\underline{d}$ , Figure V is obtained. These lines have all been drawn through the origin, and therefore apply to the case of the fixed station directly on the refracting horizon; i.e.,  $D = 0$ . The second term of equation (1) shows that the depth  $D$  from the fixed station to the refracting horizon can be taken into account by adding a constant, which is independent

of the azimuth of the shots and of the dip of the refracting horizon, to the value of the travel time given by the first term.

The procedure for analyzing travel-time data obtained from a movable station whose course is not in line with one or more fixed stations (or a spread of geophones which is not in line with one or more shots) should now be clear. From the close points one obtains the velocity  $V_1$  of the top layer. By carefully examining each travel-time curve beyond the first break, one can determine approximately the direction of dip of the lower layer. A reasonable guess is made for the value of dip  $d$  and velocity  $V_2$  of the lower layer. Using these values, Figure v is obtained as explained above. For the distance corresponding to each shot point, one picks the travel-time from Figure V, assuming zero depth for the refracting horizon beneath the fixed recording station. Thus one obtains a travel-time curve for each recording station. To each of the travel-time curves a different constant is added to achieve the best fit. This constant is equal to  $(2D \cos i)/V_1$  and enables one to solve for D, the depth to the refracting horizon. The geometry of the position in space of this refracting horizon as determined by the value of D at each recording station is checked. In practice, several different sets of values of  $V_2$ ,  $d$ , and strike have to be tried before a consistent and plausible fit is found. The more fixed stations, the more reliable the final determination of the constants.

The constants  $V_1 = 5.34$  km/sec,  $V_2 = 6.25$  km/sec,  $d = 3^\circ$  were found to give the best fit for the data of Falmouth and Mt. Desert Island, and were used in obtaining Figure V. Assuming a strike of North  $4^\circ$  West, the computed travel times and the

difference between observed and computed travel times for shots 3 through 12 at Falmouth and shots 5 through 14 at Mt. Desert Island are shown in columns 4 and 5 of Table III. The residual travel times shown in the last column of Table III are obtained by subtracting  $t_c = 0.98$  seconds to column 5 for the Falmouth data and  $t_c = 0.43$  seconds to column 5 for the Mt. Desert Island data. It appears that these residual travel times are all quite small, not exceeding 0.13 seconds.

The vertical depths to the lower layer, obtained from the formula

$$H = \frac{V_1}{2 \cos i \cos d} t_c$$

are, using the above values of  $t_c$ ,

$$H = 5.1 \text{ km, at Falmouth}$$

$$H = 2.2 \text{ km, at Mt. Desert Island.}$$

These depths are consistent with the assumed strike and slope of the 6.25 km/sec layer.

As shown in the lower section of Table III, the residual travel times for shots 13 through 15 at Falmouth and shots 1 through 4 at Mt. Desert Island are all negative, indicating that the arrival is earlier than expected on the basis of a westerly dip in the 6.25 km/sec layer. The explanation for this may lie either in a change of dip or in an underlying higher velocity layer.

The Falmouth data of shots 13 through 15 fall well along a line with an intercept of 3.4 seconds and a velocity of 7.5 km/sec. For three horizontal layers the time intercept becomes

$$t_i = \frac{2D_1}{V_1} \sqrt{1 - \left(\frac{V_1}{V_3}\right)^2} + \frac{2D_2}{V_1} \sqrt{1 - \left(\frac{V_2}{V_3}\right)^2}$$

giving 11.6 km for the thickness of the intermediate layer at Falmouth.

The Mt. Desert Island data of shots 1 through 4 do not fall along a straight line and there appears to be no way to choose between the alternative explanations of the early arrivals at Mt. Desert Island.

No consistent and conclusive interpretation of later arrivals on the seismograms has been made.

### III Mt. Desert Island to Crowell Profile

The lack of Loran and visual fixes east of Matinicus Rock (shot 13) makes the navigation of the shot boat unreliable during this portion of the traverse. As a result the error in the location of shots 14 through 30 exceeds that for shots 1 through 13. The presence of strong tides and the use of dead reckoning based upon previously determined speed make the uncertainty in the shot boat position quite large. A cumulative error in position would affect both the apparent velocity and the time intercept at Crowell. At Mt. Desert Island it would result in a travel-time curve having a different slope and intercept for the shots east and west of Matinicus Rock, as observed.

The interpretation of the Falmouth - Mt. Desert Island data given above led to the existence of a layer underlying the top layer and dipping  $3^{\circ}$  to the west. If this layer continues to the east of Matinicus Rock, the travel-time for rays refracted along this layer to the Mt. Desert Island station would also closely resemble the observed travel-time curve, at least within about 10 miles east of Matinicus Rock. At this distance the lower layer would appear at the surface, making the geometry of this simple interpretation impossible beyond shot 14. From the data obtained in this study there appears to be no way to separate the effect of a cumulative navigational error from the effect of a small regional dip in the lower layer, for the portion of the profile east of shot 14.

The original Crowell data, shown in Table II and Figure VI for shots 25 through 30, are well represented by the travel time

equation

$$T = \frac{X}{5.95 \pm .24} + 1.97$$

giving an apparent velocity of  $5.95 \pm .24$  km/sec and an intercept of 1.97 seconds.

In column 2 of Table II a correction, taking into account the known speed and direction of tidal currents,\* and assuming a negative correction of 0.5 knots to the speed of the shot boat, was applied to the positions of shots 14 through 30. These corrections resulted in bringing the lower branch of Figure IV closer to the upper one, as shown in Figure VII, and in reducing the velocity and intercept observed at Crowell as shown in Figure VI. The corrected travel time for Crowell becomes

$$T = \frac{X}{5.80} + 0.6$$

giving a velocity of 5.80 km/sec and an intercept of 0.6 seconds.

In view of the uncertainty in the navigational data and the impossibility of separating the effect of navigational error and regional structure, no conclusions on crustal structure are made on the basis of this profile.

---

\* Current Tables, Atlantic Coast, North America, 1949, p. 13,  
U. S. Department of Commerce, Coast and Geodetic Survey.

#### IV Comparison with Other Investigations

Crustal columns of North America and central Europe show (Figure VIII) a range of velocities for the superficial layer from 4.4 km/sec to 6.17 km/sec and of thicknesses from 9 km to 18 km. For the superficial layer we have found a velocity of 5.34 km/sec and a thickness of 5.2 km.

The velocities shown for the intermediate layer range from 5.95 km/sec to 7.6 km/sec, with depths to the bottom of the layer from 23 km to 40 km. For the intermediate layer we have found a velocity of 6.24 km/sec to a depth of 16.5 km. This layer may well correspond to the superficial layer found by Leet (1941), Hodgson (1947), Gutenberg (1943) to extend down to approximately 17 km.

Beneath this we have found a velocity of 7.5 km/sec, as compared with a range of 6.05 - 7.7 km/sec found by other investigations. No information on deeper layering was obtained.

One explanation, to which the result of this investigation lends support, for the relatively wide range of observed velocities and thicknesses, is the existence of a dip in the crustal layers. For lack of reverse profiles, a departure from horizontal layering could perhaps not be taken into account in most previous investigations. Such a departure from horizontal layering might become particularly appreciable near a continental margin.

## V Depth Soundings

The USS Mentor was equipped with an ultra-sonic fathometer, which obtained continuous soundings beneath the shot course across the Gulf of Maine. A plot of these soundings, shown in Figure IX A, brings out the remarkable change in bottom topography east of shot 20. While the profile is very irregular to the west of shot 20, it is smooth and has a very gentle slope to the east of shot 20. The deepest point is found near shot 25 at a depth of 520 feet.

Upon its return, the USS Mentor followed course CD, shown in Figure 1, and obtained the profile of Figure IX B. Where the return echoes from the bottom are weak and the first arrival uncertain, the profile is shown in a broken line or completely omitted.

## APPENDIX

In the plan view of Figure a, the movable shot station is up-slope and at a distance  $X$  from the fixed recording station. The bearing of the shot,  $a$ , is measured from the dip line drawn up-slope through the recording station.

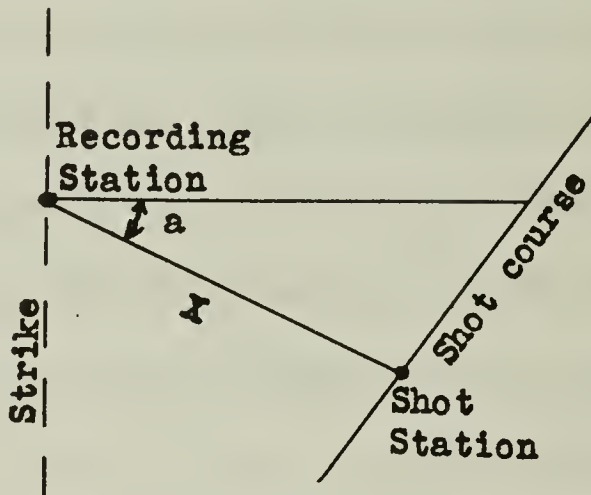


Figure a

Figure b shows the vertical plane, perpendicular to the strike of the lower layer. The upper layer has a compressional

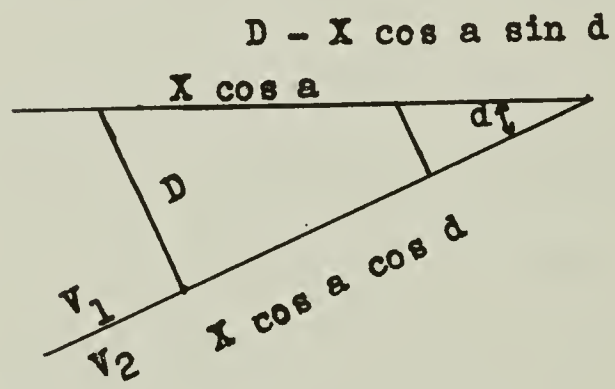


Figure b

wave velocity  $V_1$ , and the lower layer a compressional wave velocity  $V_2$  and dip angle  $d$ . The perpendicular distance from the fixed recorder to the lower layer is  $D$ . The distances shown are easily obtained from Figure a.

The projection of a portion of Figure a onto the bedding plane is shown in Figure c.

It is not difficult to show that  $\sin n = \cos a \sin d$ .  $n$  may be thought of as the apparent dip of the lower layer at bearing  $a$ .  $X \cos n$

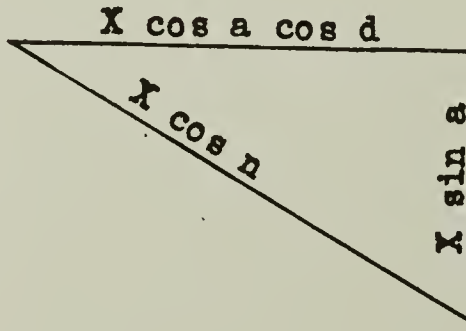


Figure c

is the shortest distance in the lower layer between the two lines which are perpendicular to the lower layer and drawn through the shot and recording stations respectively.

Combining Figures a, b, and c, Figure d shows the complete path which a critically refracted ray follows.

The critical angle of refraction  $i$  is given by  $\sin i = v_1/v_2$ . The plane of this ray is not vertical. It can be verified that the travel time for this ray is

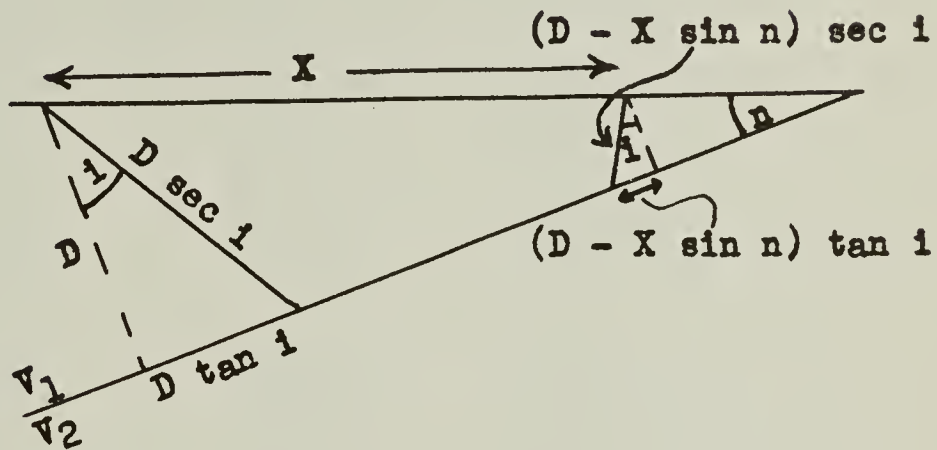


Figure d

$$T = \frac{X}{v_1} \sin(i - n) + \frac{2D \cos i}{v_1}$$

By carrying through the same construction for the shot down slope from the recorder, it can be easily shown that, except for a change of sign, the travel time remains the same. The general formula is

$$T = \frac{X}{v_1} \sin(i \pm n) + \frac{2D \cos i}{v_1} \quad (1)$$

where the plus sign is used for the fixed station up-slope from the moving station. The bearing  $a$ , the dip angle  $n$ , and therefore the apparent velocity  $v_a = v_1/\sin(i \pm n)$  all change for each shot. As explained in Section II b, the use of Figure V derived from equation (1) provides a convenient method for computing the travel time curve for a shot course at an arbitrary angle to the

strike of the lower layer. Only when the recording station is in line with the shot course and the travel time is a straight line does the constant term  $(2D \cos i)/V_1$  become the intercept of the time-axis. However, for shot distances large compared with the perpendicular distance between the shot course and the recorder, the travel time curve will approach asymptotically that which would be obtained if the recorder were in line with the shot course.

TABLE I  
Shot Times and Positions, August 11, 1949

<u>Shot No.</u>	<u>Shot Time EST</u>	<u>Shot Position</u>	
		<u>Lat. N</u>	<u>Long. W</u>
1	05:01:39.86	43°31.7'	70°01.9'
2	05:30:31.84	43°32.7'	69°55.7'
3	06:00:20.76	43°33.6'	69°49.6'
4	06:30:48.89	43°34.6'	69°43.5'
5	07:00:12.75	43°35.4'	69°37.1'
6	07:29:59.30	43°36.3'	69°31.2'
7	08:00:11.98	43°37.4'	69°25.0'
8	MISFIRE	43°38.3'	69°18.8'
9	09:00:00.29	43°39.2'	69°12.8'
10	09:30:08.63	43°40.3'	69°06.6'
11	10:00:17.95	43°41.3'	69°00.5'
12	10:30:27.89	43°42.6'	68°54.1'
13	11:00:21.38	43°43.7'	68°48.2'
14	11:30:20.23	43°43.9'	68°41.7'
15	12:00:03.39	43°44.2'	68°35.3'
16	12:30:12.40	43°44.2'	68°28.7'
17	13:00:17.62	43°44.4'	68°22.3'
18	13:30:30.58	43°44.6'	68°15.8'
19	14:00:01.89	43°44.8'	68°09.2'
20	14:30:05.79	43°44.9'	68°02.7'
21	15:00:01.44	43°45.1'	67°56.6'
22	MISFIRE	43°45.3'	67°50.5'
23	16:00:09.88	43°45.4'	67°44.5'
24	16:30:04.36	43°45.5'	67°38.5'
25	17:00:11.71	43°45.7'	67°32.4'
26	17:30:13.49	43°45.8'	67°26.1'
27	18:00:05.73	43°45.9'	67°20.0'
28	18:30:14.52	43°46.2'	67°14.0'
29	MISFIRE	43°46.2'	67°07.9'
30	19:30:32.88	43°46.3'	67°01.8'

TABLE II

Data for Falmouth, Mt. Desert Island, and Crowell Recording Stations

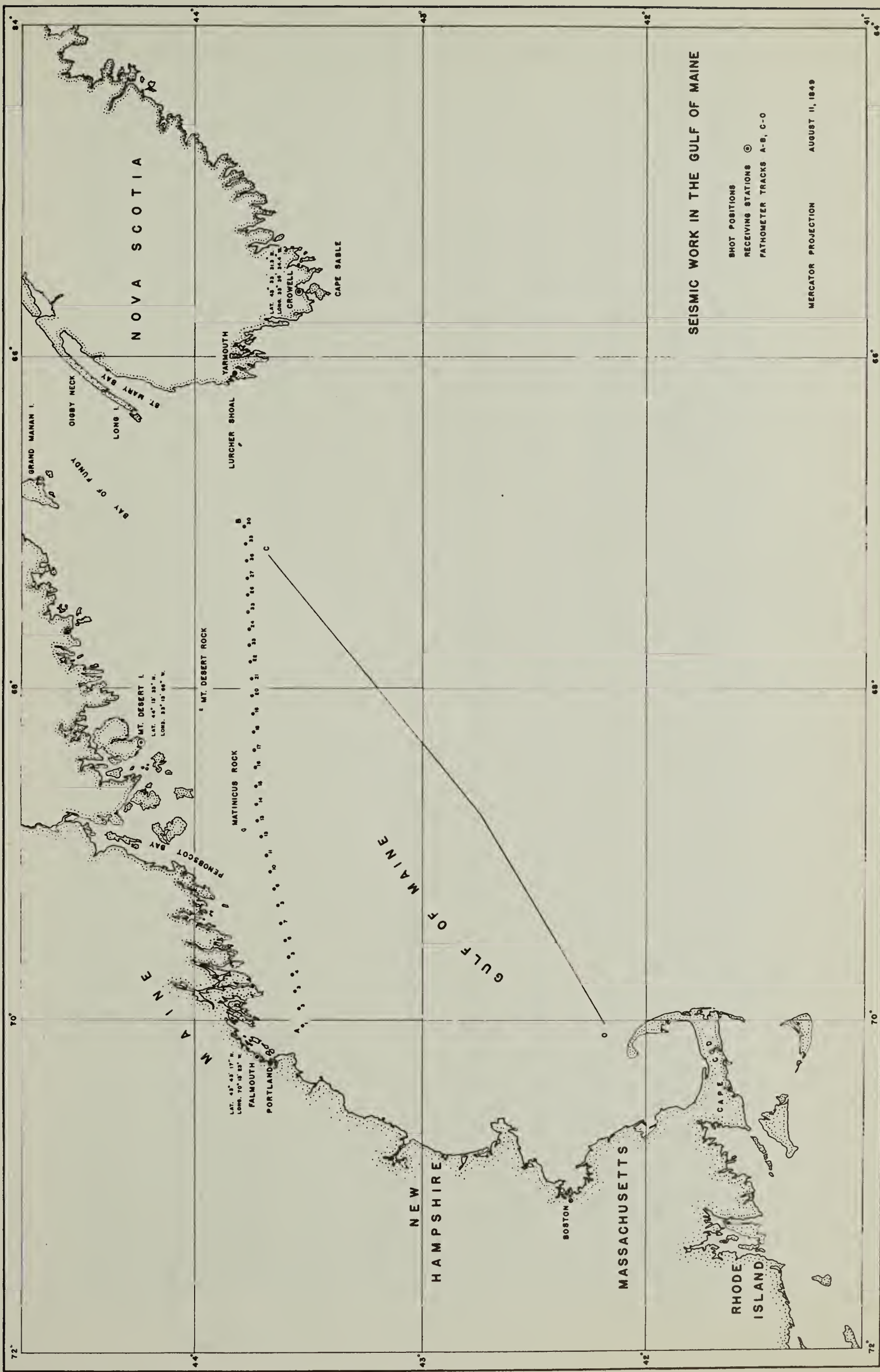
Shot No.	Falmouth, Me.			Mt. Desert Island, Me.			Crowell, N. S.		
	Travel	Corr.		Travel	Corr.		Travel	Corr.	
	Time (sec.)	Dist. N.M.	Dist. N.M.	Time (sec.)	Dist. N.M.	Dist. N.M.	Time (sec.)	Dist. N.M.	Dist. N.M.
1	4.94	14.2		26.10	85.4				
2	5.8	16.6		24.79	81.2				
3	6.67	19.8		23.59	76.8				
4	7.67	23.2		22.23	72.6				
5	8.77	27.2		21.19	68.3				
6	9.94	31.3		20.02	64.2				
7	11.08	35.2		18.85	60.2				
8	M I S F I R E			M I S F I R E					
9	13.59	43.8		16.14	52.0				
10	14.78	48.2		15.05	48.1				
11	16.08	52.6		13.98	44.3				
12	17.32	57.3		12.65	40.3				
13	18.55	61.6		11.54	36.9				
14	19.62	66.1	65.9	10.74	34.1	33.6			
15	20.83	70.8	70.4	10.07	32.0	31.0			
16				9.46	30.5	29.2			
17				9.29	29.6	28.0			
18				9.14	29.4	27.8			
19				9.27	29.9	28.4			
20				9.44	31.2	29.7			
21				9.80	33.0	31.5			
22				M I S F I R E					
23				11.12	37.9	36.4			
24				12.20	40.8	39.3			
25				13.22	44.0	42.6	28.27	84.5	86.3
26				14.30	47.3	45.8	26.91	80.1	82.05
27				15.21	50.9	49.3	25.50	75.75	77.85
28				16.19	54.6	52.9	24.20	71.5	73.75
29				M I S F I R E			M I S F I R E		
30				18.64	62.2	60.2	21.58	62.9	65.45

TABLE III  
Computed Compared with Observed Travel Times

<u>Shot No.</u>	<u>Dist. in N.M.</u>	<u>Travel Time Observed</u>	<u>Travel Time Computed</u>	<u>Observed - comp. Travel Time</u>	<u>Residual Travel Time</u>	
3	19.8	6.67	5.74	+0.93	-0.05	Falmouth, Me.
4	23.2	7.67	6.67	+1.00	+0.02	
5	27.2	8.77	7.80	+0.97	-0.01	
6	31.3	9.94	9.02	+0.92	-0.06	
7	35.2	11.08	10.09	+0.99	+0.01	
8		M I S F	I R E			
9	43.8	13.59	12.60	+0.99	+0.01	
10	48.2	14.78	13.83	+0.95	-0.03	
11	52.6	16.08	15.07	+1.01	+0.03	
12	57.3	17.32	16.44	+0.88	-0.10	
5	68.3	21.19	20.81	+0.38	-0.05	Mt. Desert
6	64.2	20.02	19.51	+0.51	+0.08	Island, Me.
7	60.2	18.85	18.27	+0.58	+0.15	
8		M I S F	I R E			
9	52.0	16.14	15.78	+0.36	-0.07	
10	48.1	15.05	14.59	+0.46	+0.03	
11	44.3	13.98	13.42	+0.56	+0.13	
12	40.3	12.65	12.20	+0.45	+0.02	
13	36.9	11.54	11.13	+0.41	-0.02	
14	34.1	10.74	10.25	+0.49	+0.06	
1	85.4	26.10	26.02	+0.08	-0.35	Mt. Desert
2	81.2	24.79	24.73	+0.06	-0.37	Island, Me.
3	76.8	23.79	23.40	+0.39	-0.04	
4	72.6	22.23	22.10	+0.13	-0.30	
13	61.6	18.55	17.65	+0.90	-0.08	Falmouth, Me.
14	66.1	19.62	18.95	+0.67	-0.31	
15	70.8	20.83	20.33	+0.50	-0.48	

## REFERENCES

1. Luskin, B., Katz, S., and Press, F., Instrumentation, Technical Reports on Seismology, No. 10, Lamont Geological Observatory (Columbia University), Jan. 1951.
2. Wald, Abraham, The Fitting of Straight Lines if Both Variables are Subject to Error, Annals of Mathematical Statistics, XI, 284-300, 1940.
3. Gutenberg, B., Travel-time Curves at Small Distances and Wave Velocities in Southern California, Gerlands Beitr. Geophysik, 35, 6, 1932.
4. Gutenberg, B., Seismological Evidence for Roots of Mountains, Bull. Geol. Soc. Am., 54, 473-498, 1943.
5. Byerly, P., Near Earthquakes in Central California, Bull. Seis. Soc. Am., 29, 427, 1939.
6. Byerly, P., and Wilson, J. T., The Central California Earthquakes of May 16, 1933 and June 17, 1934. Bull. Seis. Soc. Am., 25, 223, 1935.
7. Byerly, Perry, The Seismic Waves from the Port Chicago Explosion, Bull. Seis. Soc. Am., vol. 36, 331-348, 1946.
8. Tuve, M. A., et al., Studies of Deep Crustal Layers by Explosive Shots, Transactions, Amer. Geophysical Union, 29, 772, 1948.
9. Hodgson, J. H., Analysis of Travel Times from Rockbursts at Kirkland Lake, Ontario, Bull. Seism. Soc. Am., 37, 5, 1947.
10. Leet, L. D., Trial Travel Times for Northeastern America, Bull. Seism. Soc. Am., 31, 325, 1941.
11. Rothe, J. P., and Peterschmitt, Etude Seismique des explosions d'Haslach. Annales de l'Institut de Physique du Globe de Strasbourg, Tome V, 3ieme part., Strasbourg, 1950.
12. Willmore, P. L., Seismic Experiments on the North German Explosions 1946 to 1947, Philos. Trans. Roy. Soc. Lond., Series A, No. 843, vol. 242, 123-151, Aug. 1949.



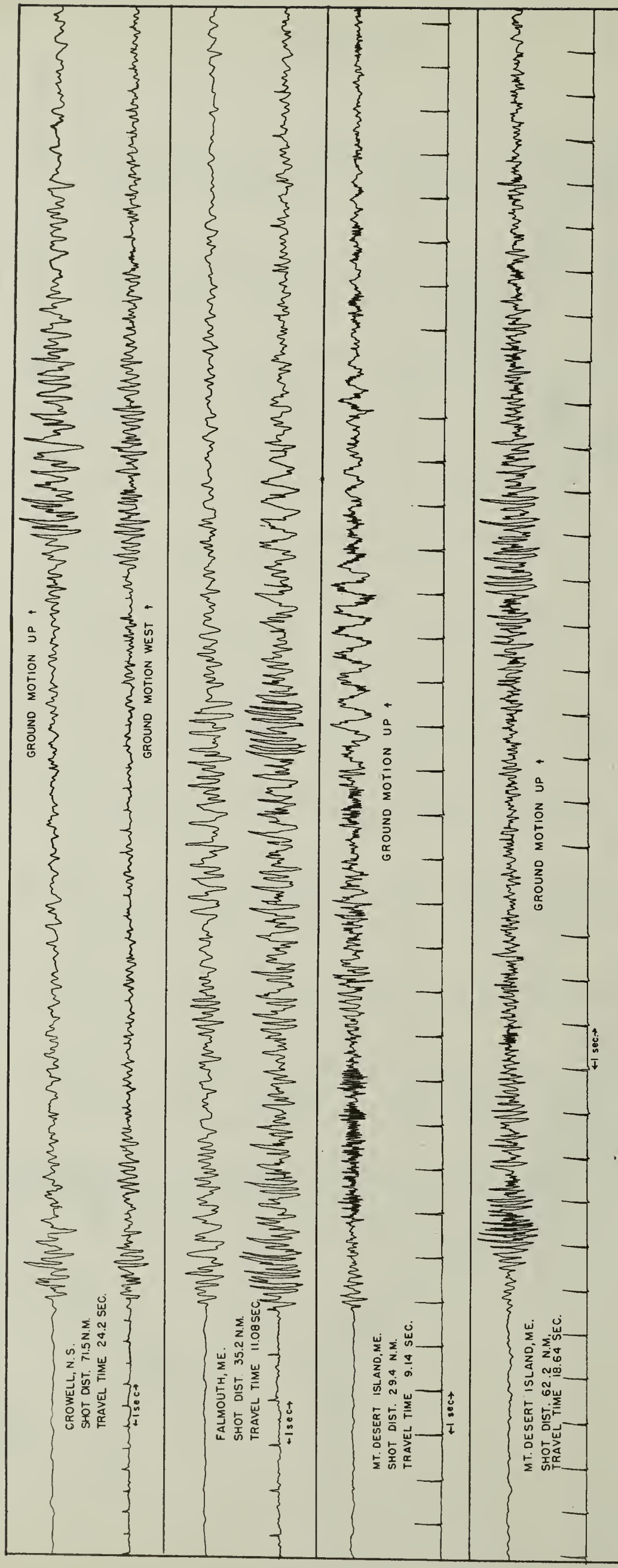
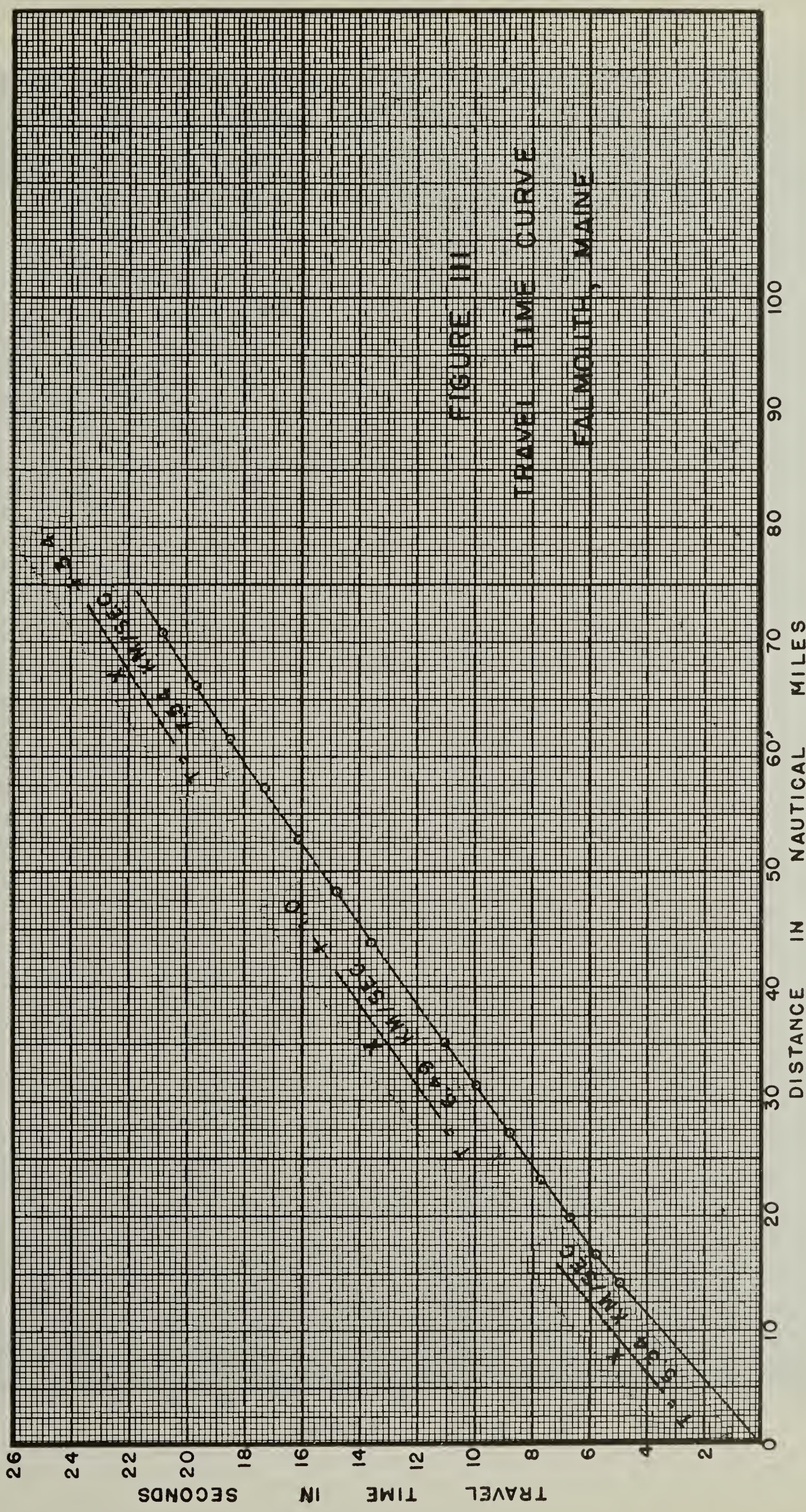
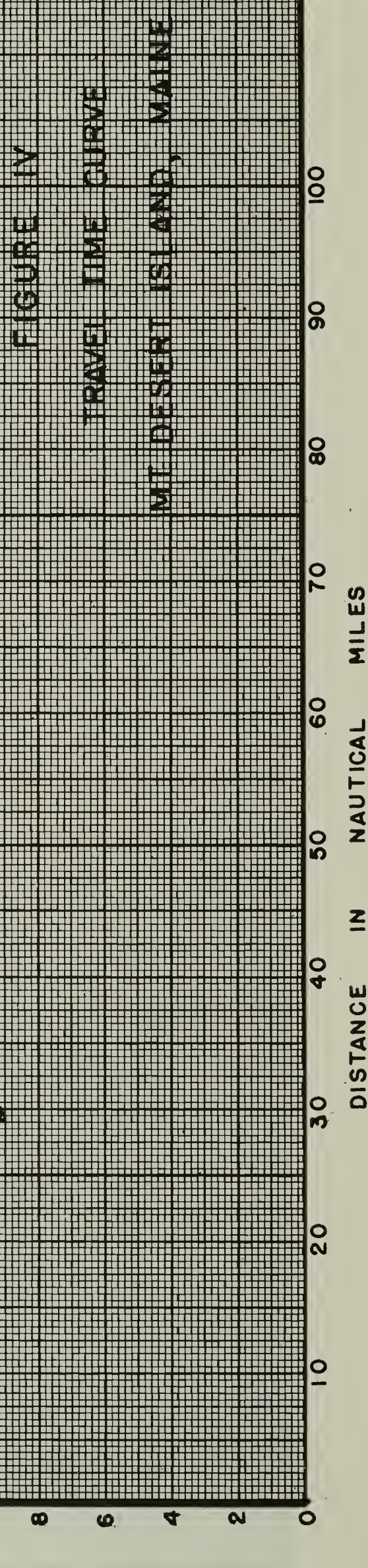
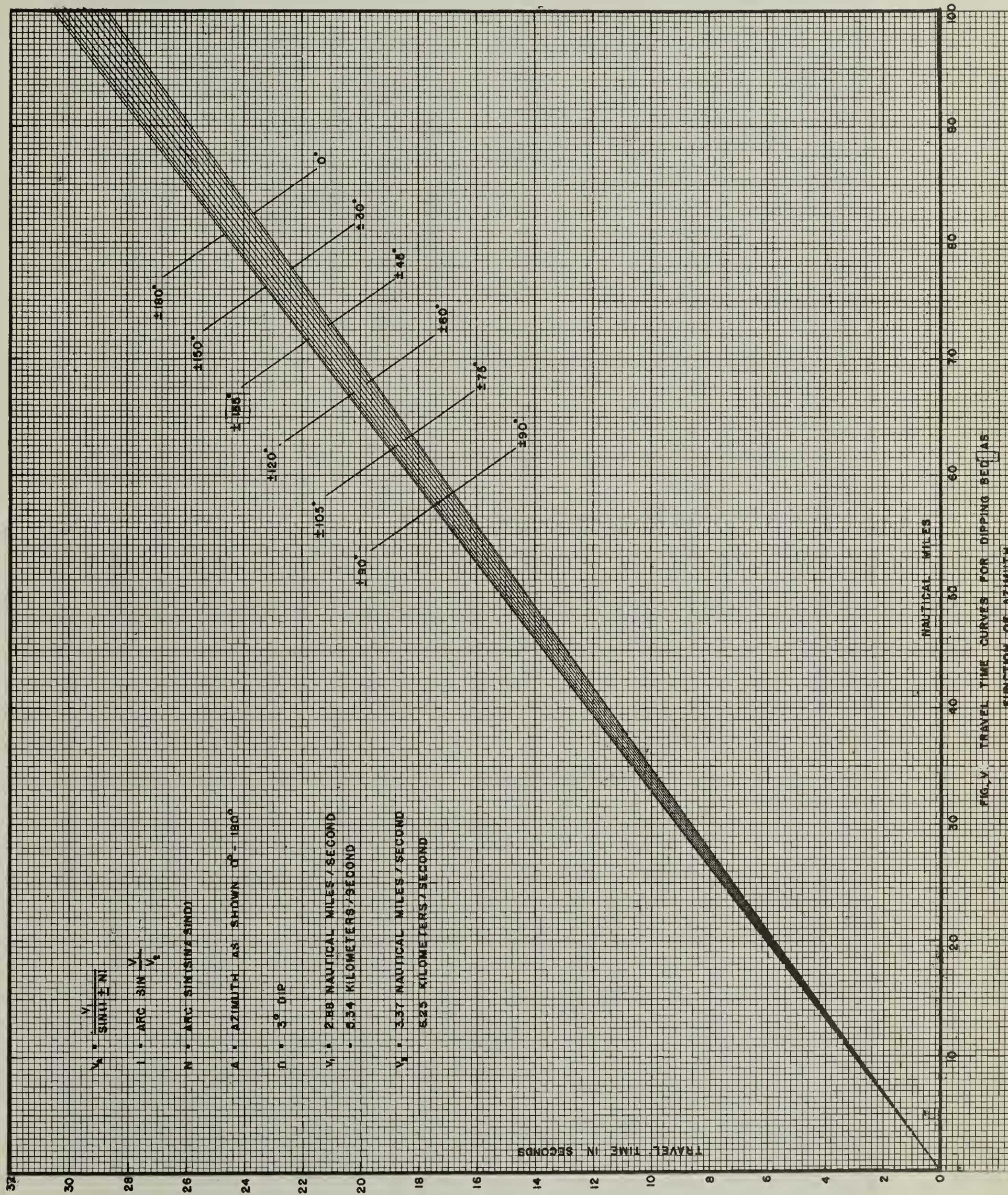
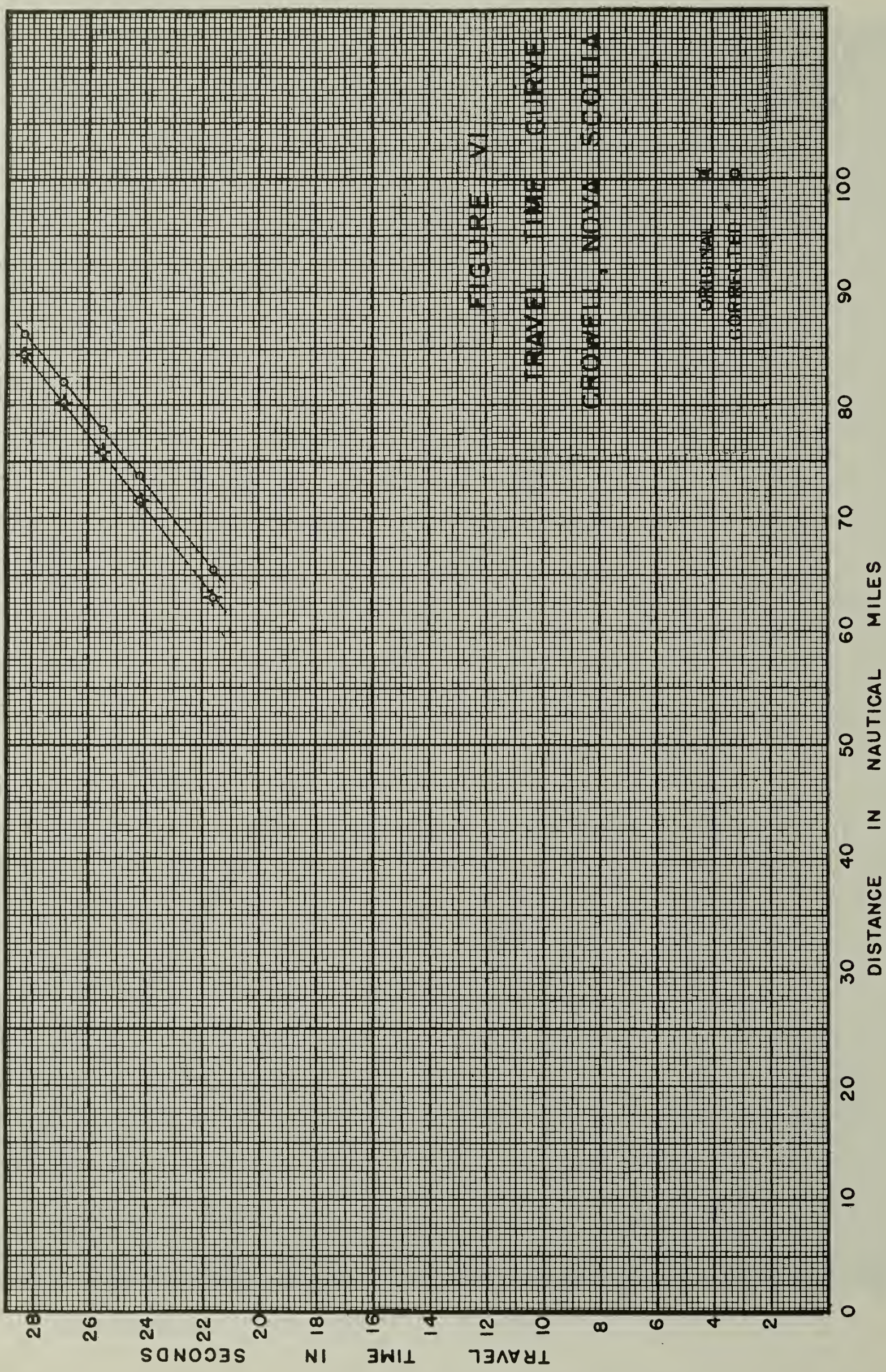


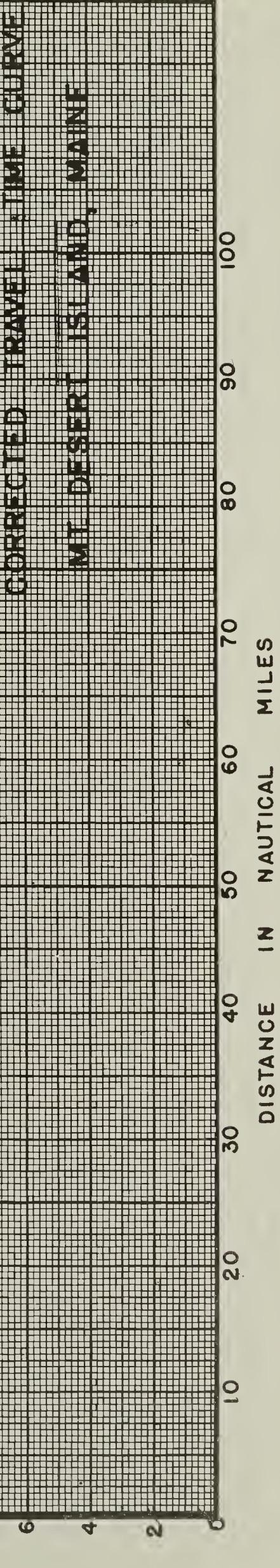
FIGURE II - SEISMOGRAMS





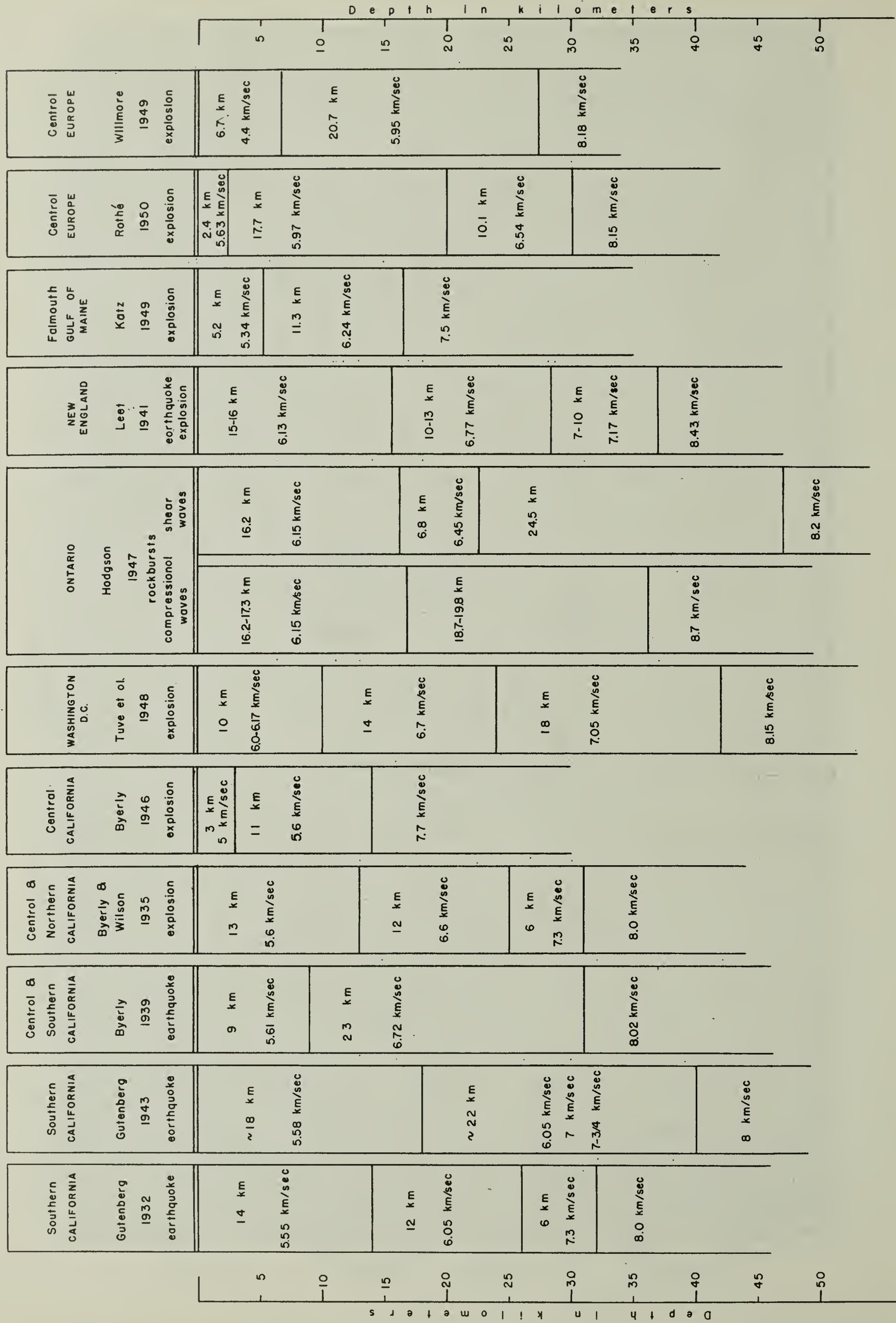


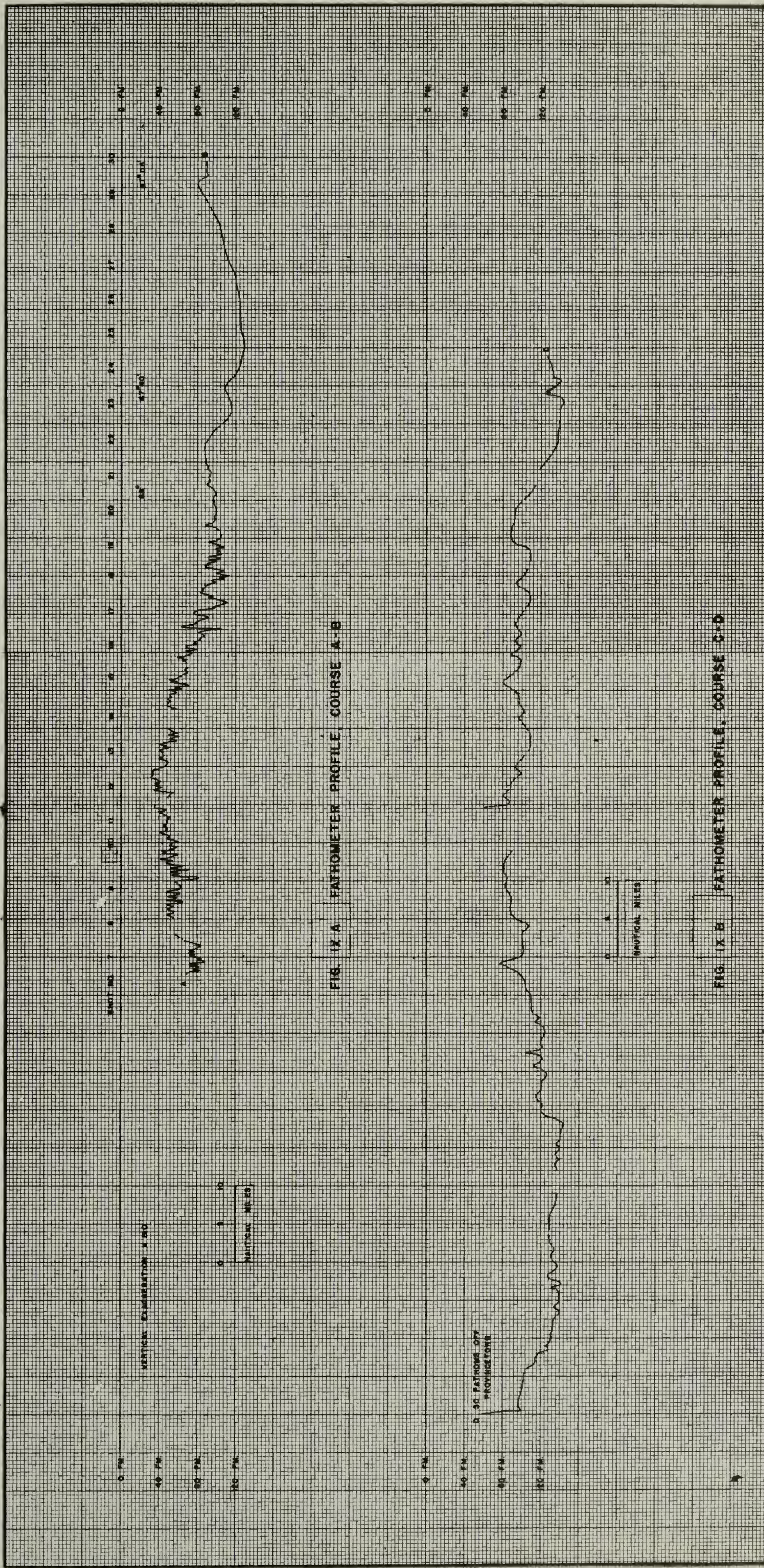




TRAVEL TIME IN SECONDS

## FIGURE VIII Crustal Columns





**FIS IX A FATHOMETER PROFILE COURSE A-B**

FIG. IX B FATHOMETER PROFILE, COURSE 3-0



COLUMBIA LIBRARIES OFFSITE



CU90645960

